Fabrication of nanoscale, high throughput, high aspect ratio freestanding gratings

Alexander Bruccoleri,[a] Pran Mukherjee, Ralf K. Heilmann, Jonathan Yam, and Mark L. Schattenburg
MIT Kavil Institute for Astrophysics and Space Research, Massachusetts Institute of Technology, Cambridge, Massachusetts 02139

Frank DiPiazza
Silicon Resources LLC, 1158 Blue Heron, Highland, Michigan 48357

(Received 28 June 2012; accepted 10 September 2012; published 5 October 2012)

A nanofabrication process has been developed for a novel critical-angle transmission grating for astronomical x-ray spectroscopy. The pitch of the gratings is 200 nm and the depth is 4 μm, which exceeds the state-of-the-art in aspect ratio by over a factor of 2 for ultrahigh aspect ratio freestanding nanoscale gratings with open areas on the order of 50% and spanning several square centimeters. They have a broad array of other applications, including neutral mass spectroscopy, ultraviolet filtration, and phase contrast imaging x-ray spectroscopy. The gratings are fabricated as a monolithic structure in silicon via two lithographic and pattern transfer processes, integrated together on a silicon-on-insulator wafer. The grating is patterned via interference lithography and transferred into the 4 μm device layer via a Bosch deep reactive-ion etch (DRIE). The grating channels are then filled without voids by spinning photoresist on them, which wicks into the channels. The sample is then bonded under vacuum via Crystal Bond™ to a carrier wafer, and a honeycomb pattern is etched via DRIE through the handle layer until it stops cleanly on the buried SiO_2. The buried SiO_2 is etched away, and the sample is separated from the carrier. The resist filling is cleaned from the channels and the grating is critical-point dried to create a freestanding structure. The freestanding gratings can now be mounted to external frames and structurally analyzed and tested for launch and deployment in space. © *2012 American Vacuum Society.*
[http://dx.doi.org/10.1116/1.4755815]

I. INTRODUCTION

This paper presents an improved process for fabricating nanoscale, ultrahigh aspect ratio freestanding gratings with high photon or particle throughput due to their large size and high open-area fractions. Specifically, the so-called critical-angle transmission (CAT) grating is targeted toward high-efficiency space-based x-ray spectrometers. In particular, there is great interest in the soft x-ray band with energies below 1 keV that covers the emission lines of carbon, nitrogen, oxygen, neon and iron.[1] Furthermore, there is a host of other potential applications including neutral mass spectroscopy,[2] ultraviolet filtration,[3] and phase contrast imaging.[4]

The CAT grating concept utilizes incident x-rays reflecting from the grating sidewalls at an angle θ_i, which is near or below the angle for total external reflection, θ_c (see Fig. 1). Diffraction occurs when the optical path length difference (OPLD) between parallel x-rays offset by one grating period is an integer multiple of the x-ray wavelength. Precisely, the OPLD for diffraction equals $2P\sin(\theta_i) = m\lambda$, and the general grating equation is

$$m\lambda = P\Big(\sin(\theta_i) + \sin(\beta_m)\Big), \tag{1}$$

where m is the diffraction order, λ is the wavelength, P is the grating period, θ_i is the angle of incidence, and β_m is the angle of the outgoing diffraction orders. The CAT grating geometry results in the outgoing x rays being channeled into diffraction orders spanning a narrow angular range, such that θ_i and β_m are similar in value. This is the so-called "blazing effect," which increases efficiency over traditional transmission gratings where most of the outgoing light is in the zeroth and plus or minus first diffraction orders. The blazed diffraction orders are centered around the angle of specular reflection. This geometry also boosts efficiency since the incoming x rays are mostly reflected due the deep channels and large open area fraction instead of either being fully transmitted in the zeroth order through vacuum without a reflection or being intercepted by the grating bars and partially absorbed. The CAT grating boosts efficiency over the state-of-the-art by a factor of 5 in the soft x-ray band.[5] Previously, state-of-the-art space-based phase-shifting x-ray transmission gratings were made of gold on a membrane and absorbed soft x rays and therefore were ineffective in that band.[6,7]

The specific dimensions for CAT gratings are set by the telescope design and desired spectral band. For example, a grating of period 200 nm, depth of 4 μm, and bar width of 40 nm can potentially provide >50% diffraction efficiency for wavelengths between 2 and 7 nm. See Fig. 2 for a computer-aided design (CAD) depiction of one CAT grating membrane cell.

The fabrication process presented here has successfully led to gratings with the desired pitch and depth, with open

[a]Electronic mail: alexbruc@mit.edu

Downloaded 15 Oct 2012 to 18.75.3.115. Redistribution subject to AVS license or copyright; see http://avspublications.org/jvstb/about/rights_and_permissions

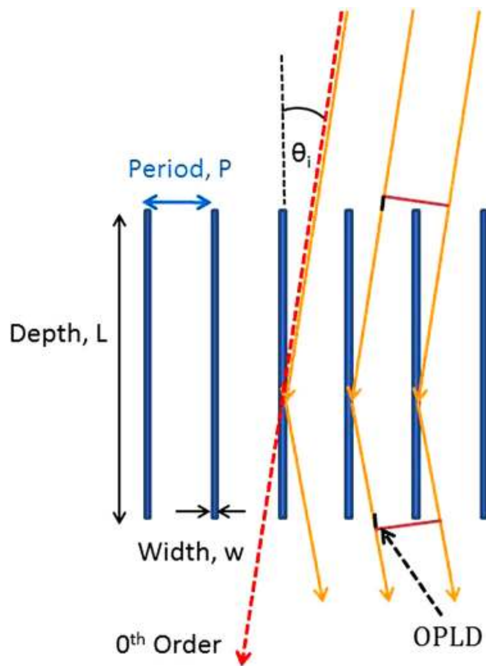

FIG. 1. (Color online) Conceptual geometric drawing of CAT grating cross section. (Not to scale.)

areas on the order of 50% and spans of several square centimeters. This more than doubles the aspect ratio of previous work on freestanding nanoscale gratings, with a period of 240 nm and a depth of 1800 nm.[8] Both of these grating fabrication processes utilize silicon-on-insulator (SOI) wafers and feature integrated structural supports in the handle and device layers. Furthermore, both processes utilize deep reactive-ion etching (DRIE) for both the SOI device and handle layer, which allows for crystal lattice independent etching.[9] The key difference is that the new process etches the device (front side) layer first as opposed to the handle (back side) layer, which allows for the deeper and more repeatable etching that is essential to achieve the ultrahigh aspect ratio of the CAT grating. A novel process step of filling the grating channels with a protective layer of photoresist allows the sample to be flipped over and etched from the back with good thermal contact. The photoresist can be cleaned after processing, enabling a freestanding grating.

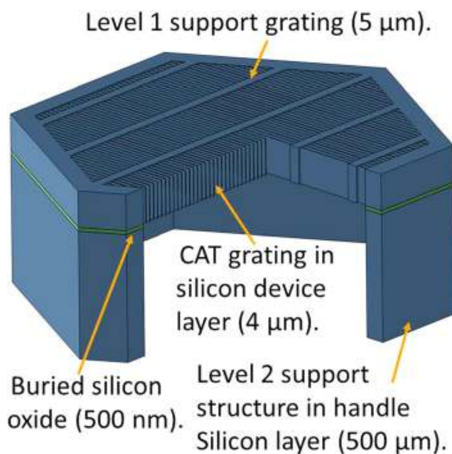

FIG. 2. (Color online) CAD depiction of one CAT grating membrane cell with structural supports. (Not to scale.)

An alternative fabrication process utilized wet-KOH etching instead of DRIE, where the CAT grating lines were patterned parallel to the vertical ⟨111⟩ planes of the ⟨110⟩ device layer. This process successfully fabricated patterns with the desired period and depth for preliminary x-ray tests; however, diagonal ⟨111⟩ planes, starting from the support structure, limited the open area fraction to ∼20%.[10,11]

II. FABRICATION METHODOLOGY

The fabrication methodology developed here for freestanding gratings is based on integrating a front and a back DRIE step on SOI wafers (see Fig. 3). A 4-μm-thick device layer is used for the CAT grating and an integrated cross support mesh designated "Level 1." The 500-nm-thick buried oxide layer acts as an etch stop for both etches, and a 500 μm handle layer serves as the source of large-area structural support designated "Level 2." The device and handle layer etches are designated "front side" and "back side," respectively. The general fabrication procedure is as follows: After substrate preparation (F1), the mask for the back side is patterned followed by front side masking (F2). The front side is then deep etched (F3), filled and protected (F4), flipped over, and bonded to a carrier wafer. The back side is then deep etched (B1), the buried layer removed (B2), and the sample is separated from the carrier, cleaned, and critical-point dried to finish (B3).

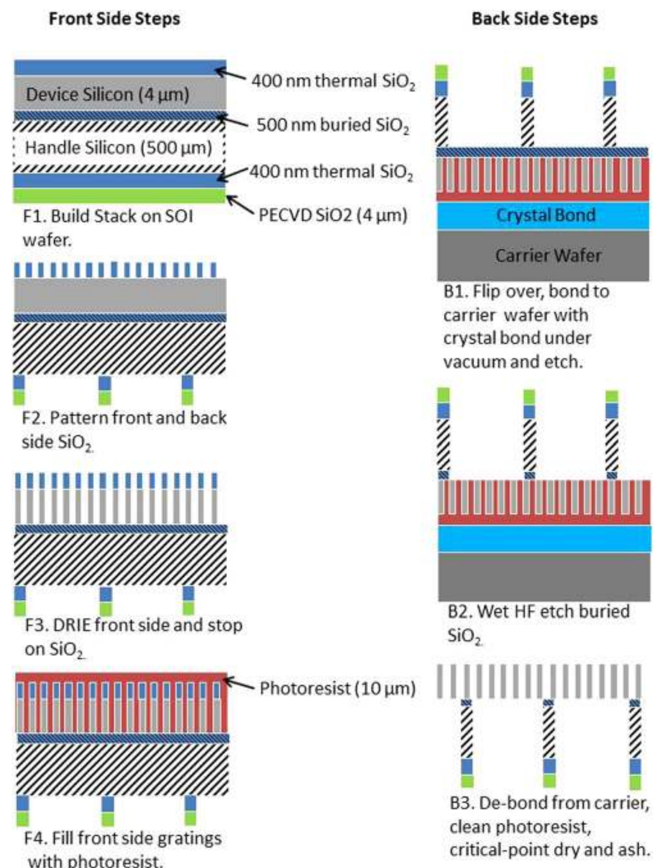

FIG. 3. (Color online) Process flow chart.

Downloaded 15 Oct 2012 to 18.75.3.115. Redistribution subject to AVS license or copyright; see http://avspublications.org/jvstb/about/rights_and_permissions

A. Front side etching

The front side is masked with 400 nm of thermal SiO_2 and etched with a rapid-cycle Bosch process in an STS Pegasus tool as demonstrated in past work.[12] This work focused on etching the CAT gratings in bulk silicon for process development. The 200-nm-pitch CAT grating pattern is created via interference lithography (IL)[13] and transferred into the 400-nm-thick thermal SiO_2 layer via a trilayer stack.[14] The Level 1 support was masked via spinning a 700-nm-layer PFI-88A7 photoresist (Sumitomo Corporation) over the patterned SiO_2. The photoresist is exposed via IL and developed with a 5 μm period and ≈20% duty cycle patterned orthogonally to the CAT grating. See Fig. 4 for a scanning electron microscope (SEM) image of the 200-nm-pitch mask prior to DRIE.

Prior etching work for 6-μm-deep CAT gratings had masking and undercutting limitations which never showed clear evidence that the etch could stop on a buried SiO_2 layer. There was some concern that charging in the buried SiO_2 could direct ions toward the grating bars and cause notching.[15] Experiments with 4 μm deep etches showed that a clean stop on SiO_2 can be achieved when using a low frequency platen power of 380 kHz. The etch parameters were the same as those presented by Mukherjee *et al.*,[12] except that the etch time was 9 min and the platen power was linearly ramped from 30 to 57 W. This etch stop is critical for patterning CAT gratings since a uniform and completely etched grating will remain after the final removal of the buried SiO_2 (see Fig. 5).

The key step that enables etching the device layer first is the fill and clean process of the CAT grating bars. *A priori* it seemed unlikely that channels ∼100 nm wide by 4 μm deep would fill with a polymer; however, they filled completely with photoresist. After back side etching, the channels are cleaned with a piranha solution. The photoresist acts purely as a strippable protective material, and it is likely that other polymers could also fill the grating channels. The specific process includes filling with two coatings of PFI-88A7 (Sumitomo Corporation) and one coat of AZ 4620 (AZ Electronic Materials) photoresist. Each coat is spun at 3000 rpm, placed in vacuum (≈0.25 atm) for outgassing and hotplate baked at 90 °C C for 60 s. With the CAT grating filled with photoresist and thus protected, the sample can be bonded to a carrier wafer for back side etching. See Fig. 5(b) for an image of the filled 4 μm deep grating. The fill and clean process has also been tested to 6 μm depth successfully. This suggests that this method can lead to gratings of much greater depths, which will enable higher energy x rays to be diffracted efficiently.

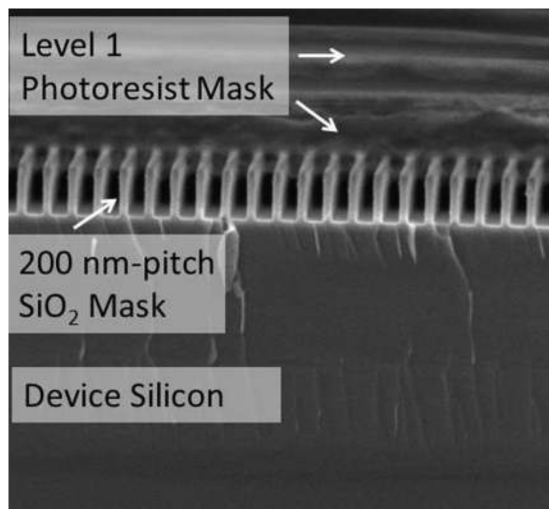

FIG. 4. Cross sectional electron micrograph of the 200-nm-pitch thermal SiO_2 mask with Level 1 cross support mask.

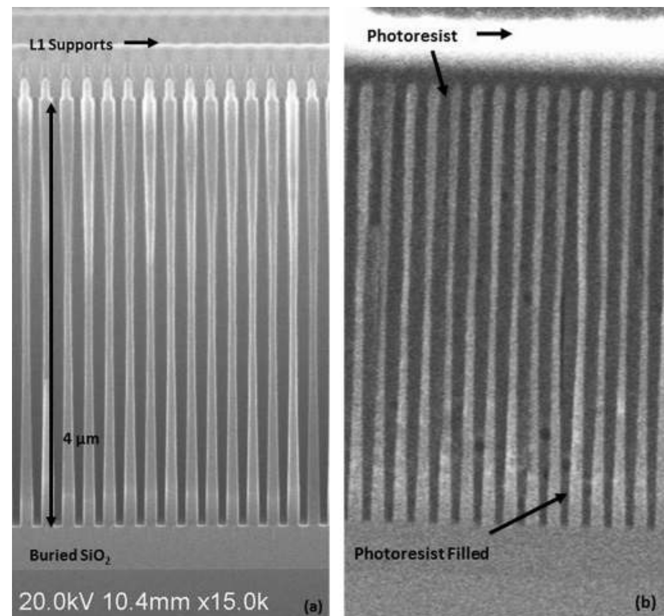

FIG. 5. Electron micrography of 200-nm-pitch CAT grating, (a) etched 4 μm deep and stopped on oxide and (b) filled with photoresist. Note the mask in Fig. 4 is the same mask used to etch the sample for (a). However, (a) and (b) are from different samples. (a) CAT grating after front side DRIE. (b) CAT grating after being filled with photoresist.

B. Back side etching

The back side etch is also performed with a Bosch process that stops on the buried oxide. The Level 2 structure comprises of 1-mm-pitch hexagons with 100-μm-wide lines, spanning 31 mm on a side (see Fig. 2 for a CAD depiction of one hexagon and Fig. 6 for a SEM image of the hexagon array). It is masked with 4 μm PECVD SiO_2 and 400 nm thermal SiO_2. The etch is not challenging as the feature sizes are large; however, uniformity is an issue. The edges of the silicon sample were observed to etch faster than the center. The likely reason is that etching near the edge can diffuse reactants and products faster than at the center. The edges of each individual millimeter-scale hexagon also etch slower than the center, leaving a circular region of etched area. This was likely due to the sidewalls shadow-masking the reactive fluorine species during the etch. These nonuniformities during the etch are acceptable since the etch can be halted, the sample removed from the tool, and the finished edges of the chip covered with protective silicon chips. This process is repeated several times until all of the hexagons are finished. This procedure protects the finished hexagons from

Downloaded 15 Oct 2012 to 18.75.3.115. Redistribution subject to AVS license or copyright; see http://avspublications.org/jvstb/about/rights_and_permissions

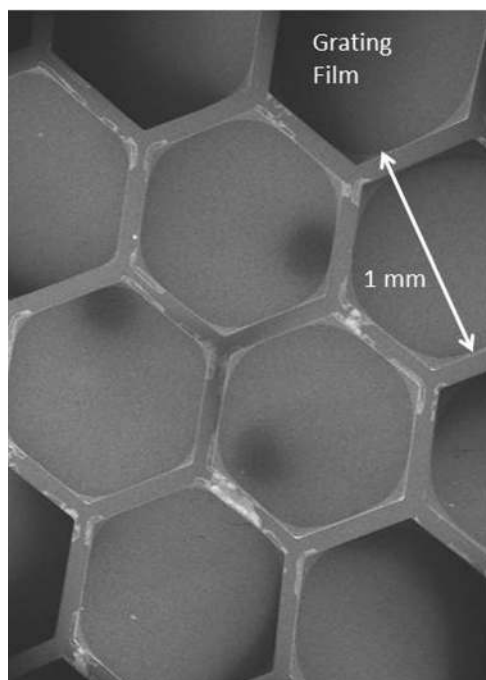

FIG. 6. Electron micrography of bottom side of hexagon support structure and grating film.

over-etching while the center hexagons finish. Furthermore, the buried SiO_2 is 500 nm thick, which allows for some etch nonuniformity before being compromised.

The back side etches are done with the sample bonded to a carrier wafer via Crystalbond 555 (Structural Probe, Inc.) using a vacuum bonding process to prevent voids in the bond. Etching nonuniformities were observed in early experiments and sometimes regions of the mask would be damaged during the etch. A likely cause is a temperature increase which diminishes the anisotropy of the etch and can undercut the mask entirely. One hypothesis for this was a poor bond to the carrier wafer, due to voids between the sample and carrier. Another hypothesis was that the $\sim$10 μm layer of photoresist impregnating the CAT grating was thermally insulating the interface between the sample and carrier wafer. A simple one-dimensional heat transfer analysis was performed to estimate the temperature rise from voids and photoresist. The approximate power through the 100-mm-diameter wafer is 1 kW. The voids were assumed to be pockets of air, and the heat transfer analysis assumed the thermal conductance to be the same as air at standard temperature and pressure (STP). The photoresist was modeled as carbon as a conservative estimate for thermal conductance. The results of the calculations are shown in Table I, which

TABLE I. Table of estimated temperature increases during etching.

Material	Thickness (μ)	Temperature rise (°C)
Silicon	500	0.5
Air (STP)	5	26
Air (STP)	50	260
Carbon	20	1.5
Carbon	10	0.75

clearly shows air pockets from voids in the bond can lead to drastic local temperature rises during etching.

To further study these results, ultrasonic imaging was taken of a damaged sample that was still bonded to a carrier. This confirmed substantial voiding under the region of poor quality etch. To address this problem, a vacuum chamber was constructed with a thermal plate to allow for chip bonding at $\sim$500 mTorr, which greatly reduces any voids in size. Ultrasonic imaging of samples bonded with this tool showed no voids, and subsequent etches were more consistent.

C. Integration and cleaning

After the back side is etched, the buried SiO_2 is removed with a wet HF etch. The chip is then immersed in water $\approx$80 °C until the Crystalbond melts and the sample floats off the carrier. The remaining photoresist is stripped from the grating channels with two successive piranha cleans. At this point, the grating bars are fragile and cannot be dried in air, since surface tension will pull them together. Instead, they are kept submerged and critical-point dried to avoid the formation of liquid–air interfaces. Finally, the sample is placed in an isotropic O_2 plasma to remove any remaining organic material within the grating bars. The result is a fully integrated CAT grating structure with Levels 1 and 2 supports. The photoresist filling is entirely removed and the grating bars are undamaged, which can be observed in SEM imagery. Sample pieces of the grating membrane were torn for SEM inspection by adhering tape to small regions, and tearing them away with tweezers such that cross sections could be imaged (see Fig. 7).

III. ANALYSIS AND DISCUSSION

The fabrication process presented here centers on processing the front side of the SOI wafer first and then finishing it with a back side etch. It has proven to be a reliable way of creating freestanding ultrahigh aspect ratio gratings. The overall span of the grating mesh is 31 by 31 mm^2 and over 80% is undamaged. Poor handling and intentional destruction for inspection damaged regions of the samples prepared thus far; however, current fabrication developments seek to minimize defects over the entire area. The duty cycle of the Level 2 hexagon is 10%, and the open area fraction is therefore $\approx$80%. The Level 1 support and CAT gratings lines prior to further processing also have an open area fraction of $\approx$80% and $\approx$50%, respectively. All of these open-area fractions can be improved; however, they demonstrate that large open areas are possible with the fabrication techniques presented. A remaining step required to realize x-ray testable CAT gratings is a wet KOH polish of the grating bars after the front side DRIE. This requires the grating bars to be aligned to the $\langle 111 \rangle$ planes as demonstrated by Ahn for purely wet etched gratings.[16] The goal is to make the CAT grating bars 40 nm thick which results in an open area fraction of 80%.

The front side process improves upon several drawbacks of a previous method developed by Mukherjee *et al.*,[8] which was also originally attempted for CAT gratings. In

Downloaded 15 Oct 2012 to 18.75.3.115. Redistribution subject to AVS license or copyright; see http://avspublications.org/jvstb/about/rights_and_permissions

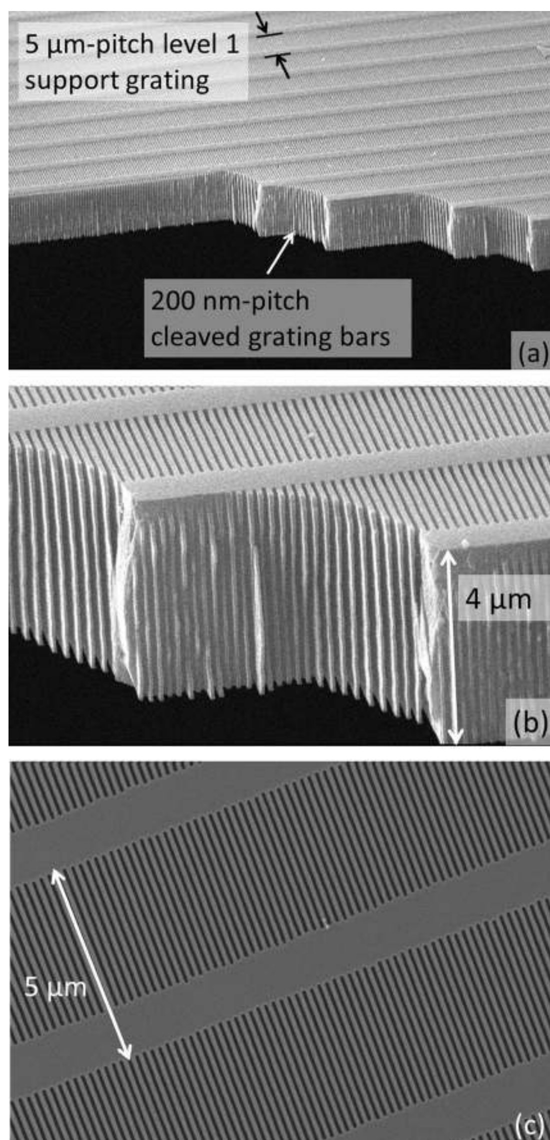

FIG. 7. Electron micrography of freestanding grating. (a) Zoomed out view of cleaved cross section of freestanding grating film. (b) Zoomed in view of cleaved cross section of freestanding grating film. (c) Back side view of grating film showing CAT grating and Level 1 support lines clearly fully etched through from above. "Wiggliness" in the lines is due to microscope vibrations. Note, (a) and (b) are from the same sample which is different than the sample for (c).

particular, the previous method processed the back side first which left millimeter-span membranes to be processed later. It required developing special carrier wafers to allow for the etch tool's helium cooling to contact the back of the membranes. This compromised control of the thermal environment of the delicate CAT grating etch, which was first developed on bulk silicon. Furthermore, any tears in any of the membranes allows helium to leak into the etch chamber, which makes process development challenging. In contrast, the etch of the CAT grating on bulk silicon during the front side first process enjoys higher thermal conductivity than helium, and more structural rigidity than a membrane. This structural stability of etching on rigid wafers is particularly important when etching CAT gratings aligned to the $\langle 111 \rangle$ planes, since any deformation of a thin membrane during etching will unalign the grating to the $\langle 111 \rangle$ planes. This is a particular problem for the process with the back side etch first since the membrane left for subsequent front side etching rests on a buried SiO_2 layer, which is under compressive stress and thus buckles and deforms significantly.

IV. CONCLUSION

A break-through fabrication process has been demonstrated to produce freestanding 200-nm-pitch CAT grating lines to a depth of 4.0 μm, which is a finer pitch and over 2.5 times the aspect ratio of the previous state-of-the-art. These gratings are ready to be structurally tested for launch and deployment in space, which includes vibration, shock, pressure, and thermal testing. The grating lines can now be aligned to the $\langle 111 \rangle$ planes for wet KOH polishing to reduce the sidewall roughness for x-ray testing.

ACKNOWLEDGMENTS

This work was funded by NASA Grants NNX08AI62G and NNX11AF30G, the MIT Kavli Institute, and the Department of Defense National Defense Science and Engineering Graduate (NDSEG) fellowship program. Specific thanks to James Daley of the MIT Nanostructures Lab, Vicky Diadiuk, Dennis Ward, Dave Terry, and Paul Tierney of the Microsystems Technology Laboratories, and Brian VanDerElzen of the University of Michigan Lurie Nanofabrication Facility.

[1]R. K. Heilmann *et al.*, Proc. SPIE **7732**, 77321J (2010).
[2]D. W. Keith, M. L. Schattenburg, H. I. Smith, and D. E. Pritchard, Phys. Rev. Lett. **61**, 1580 (1988).
[3]J. T. M. van Beek, R. C. Fleming, P. S. Hindle, J. D. Prentiss, M. L. Schattenburg, and S. Ritzau, J. Vac. Sci. Technol. B **16**, 3911 (1998).
[4]C. David, J. Bruder, T. Rohbeck, C. Grunzweig, C. Kottler, A. Diaz, O. Bunk, and F. Pfeiffer, Microelectron. Eng. **84**, 1172 (2007).
[5]R. K. Heilmann, M. Ahn, and M. L. Schattenburg, Proc. SPIE **7011**, 701106 (2008).
[6]C. R. Canizares, M. L. Schattenburg, and H. I. Smith, Proc. SPIE **597**, 253 (1986).
[7]F. Paerels, Space Sci. Rev. **157**, 15 (2010).
[8]P. Mukherjee, T. H. Zurbuchen, and L. Jay Guo, Nanotechnology **20**, 325301 (2009).
[9]G. T. A. Kovacs, N. I. Maluf, and K. E. Petersen, Proc. IEEE **86**, 1536 (1998).
[10]M. Ahn, R. K. Heilmann, and M. L. Schattenburg, J. Vac. Sci. Technol. B **25**, 2593 (2007).
[11]M. Ahn, R. K. Heilmann, and M. L. Schattenburg, J. Vac. Sci. Technol. B **26**, 2179 (2008).
[12]P. Mukherjee, A. Bruccoleri, R. K. Heilmann, M. L. Schattenburg, A. F. Kaplan, and L. J. Guo, J. Vac. Sci. Technol. B **28**, C6P70 (2010).
[13]M. L. Schattenburg, E. H. Anderson, and H. I. Smith, Phys. Scr. **41**, 13 (1990).
[14]M. L. Schattenburg, J. Vac. Sci. Technol. B **19**, 2319 (2001).
[15]F. Laermer and A. Urban, Microelectron. Eng. **67–68**, 349 (2003).
[16]M. Ahn, Ph.D. dissertation (Massachusetts Institute of Technology, 2009).

Downloaded 15 Oct 2012 to 18.75.3.115. Redistribution subject to AVS license or copyright; see http://avspublications.org/jvstb/about/rights_and_permissions